

Quantum non-demolition measurement based on an actively correlated atom-light hybrid interferometer

GAO-FENG JIAO¹, KEYE ZHANG¹, L. Q. CHEN^{1,5}, CHUN-HUA YUAN^{1,6}, AND WEIPING ZHANG^{2,3,4}

¹State Key Laboratory of Precision Spectroscopy, Quantum Institute for Light and Atoms, Department of Physics, East China Normal University, Shanghai 200062, China

²School of Physics and Astronomy, and Tsung-Dao Lee Institute, Shanghai Jiao Tong University, Shanghai 200240, China

³Shanghai Research Center for Quantum Sciences, Shanghai 201315, China

⁴Collaborative Innovation Center of Extreme Optics, Shanxi University, Taiyuan, Shanxi 030006, China

⁵Corresponding author: lqchen@phy.ecnu.edu.cn

⁶Corresponding author: chyuan@phy.ecnu.edu.cn

Compiled June 1, 2021

Quantum non-demolition (QND) measurement is an important tool in the field of quantum information processing and quantum optics. The atom-light hybrid interferometer is of great interest due to its combination of atomic spin wave and optical wave, which can be utilized for photon number QND measurement via the AC-Stark effect. In this paper, we present an actively correlated atom-light hybrid interferometer where the output is detected with the method of active correlation output readout via a nonlinear Raman process (NRP). Then this interferometer is used for QND measurement of photon number and the signal-to-noise ratio (SNR) is studied. Compared to the traditional SU(2) interferometer, the SNR in a balanced case is improved by a gain factor of g of NRP. Furthermore, the performance of QND measurement is analyzed. In the presence of losses, the measurement quality is reduced. We can adjust the gain parameter of the NRP in readout stage to reduce the impact due to losses. Moreover, this scheme is a multiarm interferometer, which has the potential of multiparameter estimation with many important applications in the detection of vector fields, quantum imaging and so on.

© 2021 Optical Society of America

<http://dx.doi.org/10.1364/ao.XX.XXXXXX>

1. INTRODUCTION

Quantum measurement takes place at the interface between the quantum world and macroscopic reality. According to quantum mechanics, as soon as we observe a system we actually perturb it. Quantum non-demolition (QND) measurement aims to evade the back action noise arising from the measurement [1, 2], which has given us a window on a variety of quantum systems, including mechanical oscillators [3, 4], trapped ions [5, 6], solid-state spin qubits [7, 8], circuit quantum electrodynamics [9, 10], and photons [11, 12].

In the quantum optics community, Imoto *et al.* [13] proposed an optical interferometer for QND measurement scheme of the photon number using the optical Kerr effect, in which the cross-Kerr interaction encodes the photon number of the signal state onto a phase shift of the probe state. Subsequently, some works about the photon number QND measurement are studied [14–19]. However, the main obstacles to optical QND measurement using cross-phase modulation based on third-order nonlinear

susceptibilities $\chi^{(3)}$ are the small value of nonlinearity in the available media and the absorption of photons. Munro *et al.* [20] presented an implementation of the QND measurement scheme with the required nonlinearity provided by the giant Kerr effect achievable with AC-Stark electromagnetically transparency. In addition, the schemes using cavity or circuit quantum electrodynamical systems have enabled photon number QND measurements that do not rely on the material nonlinearity through strong light-matter interactions [21–25].

Recently, the atom-light hybrid interferometer has drawn considerable interest because it is sensitive to both optical and atomic phase shift [26–31]. There are two types of atom-light hybrid interferometers, which have been also demonstrated experimentally by our group. The first type is the SU(2) linear interferometer with linear Raman process (LRP) replacing regular beam splitter for linear superposition of atomic wave and optical wave [28]. The second type is the SU(1,1) nonlinear interferometer utilizing nonlinear Raman process (NRP) for wave split-

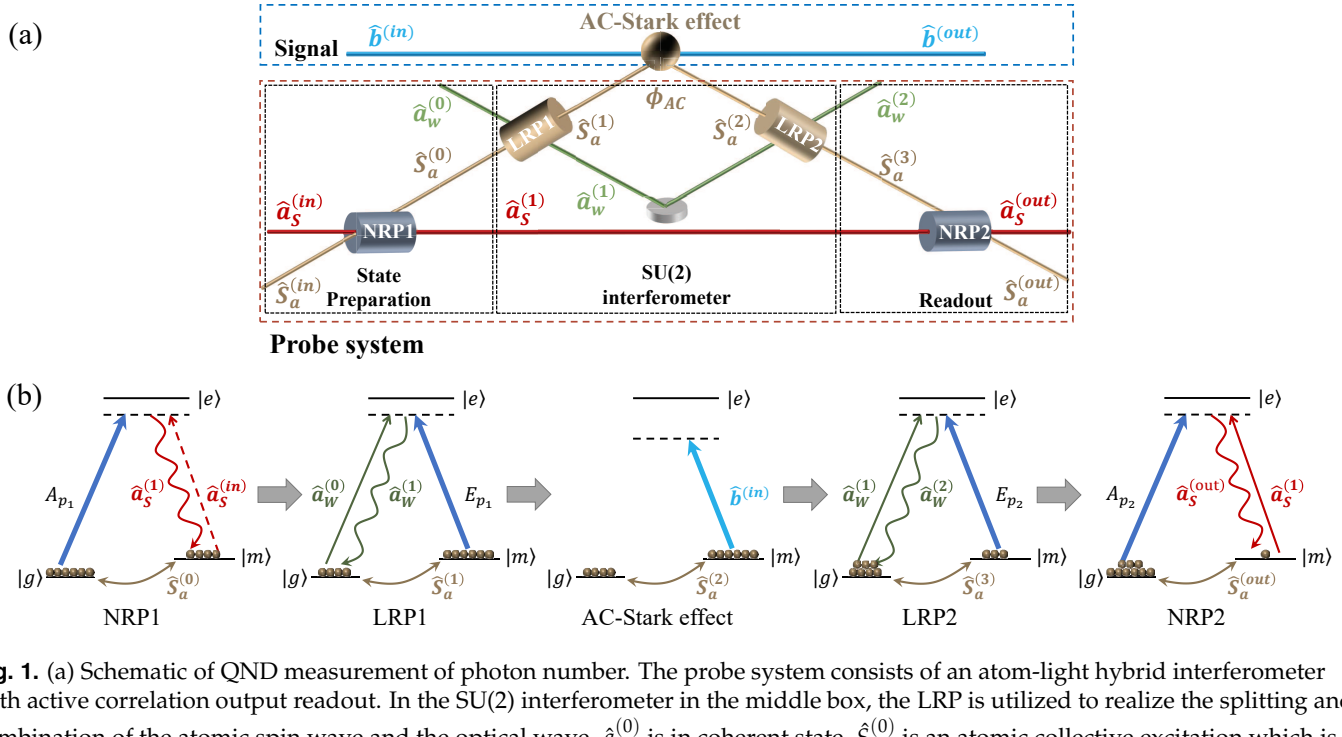


Fig. 1. (a) Schematic of QND measurement of photon number. The probe system consists of an atom-light hybrid interferometer with active correlation output readout. In the SU(2) interferometer in the middle box, the LRP is utilized to realize the splitting and combination of the atomic spin wave and the optical wave. $\hat{a}_W^{(0)}$ is in coherent state, $\hat{S}_a^{(0)}$ is an atomic collective excitation which is prepared by the NRP1. The atomic spin wave $\hat{S}_a^{(1)}$ experiences a phase modulation ϕ_{AC} via the AC-Stark effect by signal light $\hat{b}^{(in)}$. The generated atomic spin wave $\hat{S}_a^{(3)}$ of the SU(2) interferometer and the optical wave $\hat{a}_S^{(1)}$ which is correlated with $\hat{S}_a^{(0)}$ are combined to realize active correlation output readout via the NRP2. LRP, linear Raman process; NRP, nonlinear Raman process. (b) Energy levels of the atom. The lower two energy states $|g\rangle$ and $|m\rangle$ are the hyperfine split ground states. The higher-energy state $|e\rangle$ are the excited state. The strong pump beams A_{p1} (A_{p2}) and E_{p1} (E_{p2}) couple the transitions $|g\rangle \rightarrow |e\rangle$ and $|m\rangle \rightarrow |e\rangle$, respectively. $\hat{b}^{(in)}$ is far off resonance with the transition $|m\rangle \rightarrow |e\rangle$ by a large detuning.

ting and recombination [29]. This new type interferometer can be applied to QND measurement of photon number based on the AC-Stark effect [32, 33]. However, due to the requirements of detection of laser source stability in LIGO, the intensity stabilization justments are very strict across the gravitational wave band [34] and higher accuracy is required for QND measurement of high photon number.

In this paper, we present an actively correlated atom-light hybrid interferometer, which is combination of SU(2) and SU(1,1) type atom-light hybrid interferometers. We theoretically study the SNR and estimate the quality of this scheme as a QND measurement using the criteria introduced by Holland *et al.* [35], and the condition for a perfect correlation is given. In the presence of losses, the measurement quality is reduced. However, we can adjust the gain parameter of the NRP in readout stage to reduce the impact due to losses. Compared to the previous works [32, 33], the actively correlated atom-light hybrid interferometer can be realized QND measurement of photon number with higher precision.

2. ATOM-LIGHT HYBRID INTERFEROMETER WITH ACTIVE CORRELATION OUTPUT READOUT

The schematic of QND measurement of photon number is shown in Fig. 1(a). The probe system consists of an actively correlated atom-light hybrid interferometer, and when the atoms are illuminated by the off-resonant signal light $\hat{b}^{(in)}$, the interaction between atom and light will lead to an AC-Stark shift in

atomic level without atomic absorption. The energy levels of atom are given in Fig. 1(b). In the NRP1 (NRP2) and LRP1 (LRP2), the strong pump beams A_{p1} (A_{p2}) and E_{p1} (E_{p2}) couple the transitions $|g\rangle \rightarrow |e\rangle$ and $|m\rangle \rightarrow |e\rangle$, respectively. $|g\rangle$ and $|m\rangle$ are the hyperfine split ground states, $|e\rangle$ denotes the excited state. We can express the output operators of the probe system as a function of the input operators in three steps: the state preparation, the SU(2) interferometer, the readout. In the first step, we prepare the initial atomic spin wave $\hat{S}_a^{(0)}$ and a correlated optical wave $\hat{a}_S^{(1)}$ via the NRP1. It can be described as

$$\hat{S}_a^{(0)} = G_1 \hat{S}_a^{(in)} + g_1 e^{i\theta_1} \hat{a}_S^{(in)}, \quad \hat{a}_S^{(1)} = G_1 \hat{a}_S^{(in)} + g_1 e^{i\theta_1} \hat{S}_a^{(in)}, \quad (1)$$

where $e^{i\theta_1} = \eta A_{p1} / |\eta A_{p1}|$, A_{p1} is the amplitude of the pump beam and η is the coupling constant. $G_1 = \cosh(|\eta A_{p1}| \tau)$ and $g_1 = \sinh(|\eta A_{p1}| \tau)$ are the gains of the NRP1 with $G_1^2 - g_1^2 = 1$, τ is the pulse duration of pump beam.

Next, the beam splitter in a SU(2) interferometer is provided by the LRP, which can split and mix the atomic spin wave and the optical wave coherently for interference. When the atoms are illuminated by an off-resonant signal light $\hat{b}^{(in)}$, the atomic spin wave $\hat{S}_a^{(1)}$ experiences an AC-Stark shift ϕ_{AC} [36, 37]. $\hat{a}_W^{(0)}$ is in coherent state, $\hat{S}_a^{(0)}$ is an atomic collective excitation which is prepared by the NRP1. The relationship between input and output in the SU(2) interferometer is given by

$$\hat{S}_a^{(3)} = t \hat{S}_a^{(0)} + r \hat{a}_W^{(0)}, \quad \hat{a}_W^{(2)} = t \hat{a}_W^{(0)} + r \hat{S}_a^{(0)}, \quad (2)$$

where $t = e^{i\phi/2} \cos(\phi/2)$, $r = ie^{i\phi/2} \sin(\phi/2)$. ϕ includes the phase difference ϕ_0 of the interferometer and the phase difference ϕ_{AC} caused by the AC-Stark effect with $\phi_{AC} = \kappa \hat{n}_b$ [36, 37], κ and \hat{n}_b are the AC-Stark coefficient and photon number operator of the signal light $\hat{b}^{(in)}$, respectively.

In the final step, the generated atomic spin wave $\hat{S}_a^{(3)}$ of the SU(2) interferometer and the optical wave $\hat{a}_S^{(1)}$ are combined to realize active correlation output readout via the NRP2. It can be expressed as

$$\hat{S}_a^{(out)} = G_2 \hat{S}_a^{(3)} + g_2 e^{i\theta_2} \hat{a}_S^{\dagger(1)}, \quad \hat{a}_S^{(out)} = G_2 \hat{a}_S^{(1)} + g_2 e^{i\theta_2} \hat{S}_a^{\dagger(3)}, \quad (3)$$

where $e^{i\theta_2} = \eta A_{p_2} / |\eta A_{p_2}|$, A_{p_2} is the amplitude of the pump beam and η is the coupling constant. $G_2 = \cosh(|\eta A_{p_2}| \tau)$ and $g_2 = \sinh(|\eta A_{p_2}| \tau)$ are the gains of the NRP2 with $G_2^2 - g_2^2 = 1$.

And thus, the full input-output relation of the actively correlated atom-light hybrid interferometer is

$$\begin{aligned} \hat{a}_S^{(out)} &= A \hat{a}_S^{(in)} + B \hat{S}_a^{\dagger(1)} + C \hat{a}_W^{\dagger(0)}, \\ \hat{S}_a^{(out)} &= D \hat{a}_S^{\dagger(1)} + E \hat{S}_a^{(in)} + F \hat{a}_W^{(0)}, \end{aligned} \quad (4)$$

where

$$\begin{aligned} A &= G_2 G_1 + g_2 g_1 e^{i(\theta_2 - \theta_1)} t^*, \\ B &= G_2 g_1 e^{i\theta_1} + G_1 g_2 e^{i\theta_2} t^*, \\ D &= G_1 g_2 e^{i\theta_2} + G_2 g_1 e^{i\theta_1} t, \\ E &= g_2 g_1 e^{i(\theta_2 - \theta_1)} + G_2 G_1 t, \\ C &= g_2 e^{i\theta_2} r^*, F = G_2 r. \end{aligned} \quad (5)$$

3. QND MEASUREMENT OF PHOTON NUMBER

A. SNR analysis

SNR analysis is helpful to examine the performance of the QND measurement process. Given the homodyne detection, the SNR is defined as

$$R = \frac{\langle \hat{X}_S^{(out)} \rangle^2}{\Delta^2 \hat{X}_S^{(out)}}, \quad (6)$$

where $\langle \hat{X}_S^{(out)} \rangle$ and $\Delta^2 \hat{X}_S^{(out)}$ denote the quantum expectation and variance of the amplitude quadrature, respectively. In our scheme, they are given by

$$\begin{aligned} \langle \hat{X}_S^{(out)} \rangle &= \langle \hat{a}_S^{(out)} + \hat{a}_S^{\dagger(out)} \rangle \\ &= g_2 N_\alpha^{1/2} [\cos(\theta_2 - \theta_\alpha - \phi) - \cos(\theta_2 - \theta_\alpha)]. \end{aligned} \quad (7)$$

$$\begin{aligned} \Delta^2 \hat{X}_S^{(out)} &= G_2^2 G_1^2 + G_2^2 g_1^2 + g_2^2 (1 - \cos \phi) / 2 \\ &\quad + g_2^2 g_1^2 (1 + \cos \phi) / 2 + G_1^2 g_2^2 (1 + \cos \phi) / 2 \\ &\quad + 2 G_2 G_1 g_2 g_1 \cos(\theta_2 - \theta_1 - \phi) \\ &\quad + 2 G_2 G_1 g_2 g_1 \cos(\theta_2 - \theta_1). \end{aligned} \quad (8)$$

Here $\hat{a}_S^{(in)}$ and $\hat{S}_a^{(in)}$ are in vacuum states, $\hat{a}_W^{(0)}$ is in a coherent state $|\alpha\rangle$ with $\alpha = N_\alpha^{1/2} e^{i\theta_\alpha}$ where N_α and θ_α are the photon number and initial phase of the coherent state, respectively. Under the condition of $\theta_1 = 0$, $\theta_2 = \pi$, $\theta_\alpha = \pi/2$, and $\phi_0 = 0$ with a small ϕ_{AC} around ϕ_0 , assuming the signal light is in a number state $|n\rangle$ with $\hat{n}_b |n\rangle = n_b |n\rangle$ and substituting ϕ_{AC} with $\kappa \hat{n}_b$, Eq. (7) and Eq. (8) are rewritten in terms of n_b , such that

$$\langle \hat{X}_S^{(out)} \rangle = g_2 \kappa N_\alpha^{1/2} n_b, \quad (9)$$

and

$$\Delta^2 \hat{X}_S^{(out)} = (G_2 G_1 - g_2 g_1)^2 + (G_2 g_1 - g_2 G_1)^2 + G_1^2 g_2^2 \kappa^2 n_b^2 / 2, \quad (10)$$

respectively.

Considering a balanced case $G_2 = G_1 = G$ and $g_2 = g_1 = g$, the SNR is approximately $g^2 \kappa^2 N_\alpha n_b^2$. To have single-photon resolution, we need AC-Stark coefficient $\kappa \sim 1/g N_\alpha^{1/2}$. Compared to the traditional SU(2) interferometer [32], the required coefficient is smaller by a factor of $1/g$. This is due to the method of active correlation output readout for the SU(2) interferometer [38], in which the SNR is greater than the SU(2) interferometer by a factor of g of NRP.

B. Quality estimation

In this section, we estimate the quality of the actively correlated atom-light hybrid interferometer as a QND measurement using the criteria introduced by Holland *et al.* [35], which are

$$C_{S^{in} S^{out}}^2 = \frac{|\langle S^{in} S^{out} \rangle - \langle S^{in} \rangle \langle S^{out} \rangle|^2}{\Delta^2 S^{in} \Delta^2 S^{out}}, \quad (11)$$

$$C_{S^{in} P^{out}}^2 = \frac{|\langle S^{in} P^{out} \rangle - \langle S^{in} \rangle \langle P^{out} \rangle|^2}{\Delta^2 S^{in} \Delta^2 P^{out}}, \quad (12)$$

$$C_{S^{out} P^{out}}^2 = \frac{|\langle S^{out} P^{out} \rangle - \langle S^{out} \rangle \langle P^{out} \rangle|^2}{\Delta^2 S^{out} \Delta^2 P^{out}}, \quad (13)$$

with

$$\begin{aligned} \Delta^2 S^{in} &= \langle (S^{in})^2 \rangle - \langle S^{in} \rangle^2, \\ \Delta^2 S^{out} &= \langle (S^{out})^2 \rangle - \langle S^{out} \rangle^2, \\ \Delta^2 P^{in} &= \langle (P^{in})^2 \rangle - \langle P^{in} \rangle^2, \\ \Delta^2 P^{out} &= \langle (P^{out})^2 \rangle - \langle P^{out} \rangle^2, \end{aligned} \quad (14)$$

where S^{in} is the input signal incident on the scheme and P^{out} is the output probe measured by a detector. Here S^{in} is the photon number of the input signal $\hat{N}^{(in)} = \hat{b}^{\dagger(in)} \hat{b}^{(in)}$, and the probe is the amplitude quadrature $\hat{X}_S^{(out)}$. Eq. (11) is about how much the probe system degrades the signal of the measured system. Eq. (12) is about how good the probe system is a measurement device. Eq. (13) is that how good the probe system is a state preparation device. For a ideal QND measurement device the correlation coefficients $C_{S^{in} S^{out}}^2$, $C_{S^{in} P^{out}}^2$ and $C_{S^{out} P^{out}}^2$ are unity. In our paper, the signal light leading to the AC-Stark shift is far off resonance with a large detuning, i.e., the photon number of the measured signal light is not changed before and after measurement. So the first criterion is satisfied, the second and the third criteria become same: $C_{\hat{N}^{(in)} \hat{X}_S^{(out)}}^2 = C_{\hat{N}^{(out)} \hat{X}_S^{(out)}}^2$, that is,

$$C^2 = \frac{|\langle \hat{N}^{(in)} \hat{X}_S^{(out)} \rangle - \langle \hat{N}^{(in)} \rangle \langle \hat{X}_S^{(out)} \rangle|^2}{\Delta^2 \hat{N}^{(in)} \Delta^2 \hat{X}_S^{(out)}}. \quad (15)$$

For brevity, we omit the subscript of C . We obtain

$$\begin{aligned} \langle \hat{N}^{(in)} \rangle &= N_\beta, \quad \Delta^2 \hat{N}^{(in)} = N_\beta, \\ \langle \hat{X}_S^{(out)} \rangle &= g_2 \kappa N_\alpha^{1/2} N_\beta, \quad \langle \hat{N}^{(in)} \hat{X}_S^{(out)} \rangle = g_2 \kappa N_\alpha^{1/2} N_\beta (N_\beta + 1), \\ \Delta^2 \hat{X}_S^{(out)} &= (G_2 G_1 - g_2 g_1)^2 + (G_2 g_1 - g_2 G_1)^2 \\ &\quad + g_2^2 \kappa^2 N_\alpha N_\beta + G_1^2 g_2^2 \kappa^2 N_\beta (N_\beta + 1) / 2. \end{aligned} \quad (16)$$

Here the signal light is in a coherent state $|\beta\rangle$ with photon number N_β . Substituting Eq. (16) into Eq. (15), the criteria can be written as

$$C^2 = \frac{1}{1 + \frac{(G_2 G_1 - g_2 g_1)^2 + (G_2 g_1 - G_1 g_2)^2}{g_2^2 \kappa^2 N_\alpha N_\beta} + \frac{G_1^2 (N_\beta + 1)}{2 N_\alpha}}. \quad (17)$$

As seen in Eq. (17), a perfect correlation $C^2 \approx 1$ can be satisfied under the condition of $g_2^2 \kappa^2 N_\alpha N_\beta \gg (G_2 G_1 - g_2 g_1)^2 + (G_2 g_1 - G_1 g_2)^2$ and $2 N_\alpha \gg G_1^2 (N_\beta + 1)$. In a balanced case, the condition for a perfect correlation is $g^2 \kappa^2 N_\alpha N_\beta \gg 1$ and $2 N_\alpha \gg G^2 (N_\beta + 1)$.

C. Optimized C in the presence of losses

Next, we investigate the effects of losses on the correlation coefficient C consisting of photon losses and atomic decoherence losses [31].

The loss of the two arms inside the SU(2) interferometer is called the internal loss, as shown in Fig. 2(a). The loss at the output of SU(2) and the associated optical field is called external loss, as shown in Fig. 2(b). Two fictitious beam splitters are introduced to mimic the loss of photons into the environment, then the optical waves $\hat{a}_W^{(1)}$ and $\hat{a}_S^{(1)}$ experience losses as

$$\hat{a}_{W,l}^{(1)} = \sqrt{\eta_1} \hat{a}_W^{(1)} + \sqrt{1 - \eta_1} \hat{V}_1, \quad (18)$$

$$\hat{a}_{S,l}^{(1)} = \sqrt{\eta_2} \hat{a}_S^{(1)} + \sqrt{1 - \eta_2} \hat{V}_2, \quad (19)$$

where subscript l indicates the loss, η_1 (η_2) and \hat{V}_1 (\hat{V}_2) represent the transmission rate and vacuum, respectively. The spin waves $\hat{S}_a^{(2)}$ and $\hat{S}_a^{(3)}$ also undergo the collisional dephasing $e^{-\Gamma_1 \tau_1}$ ($e^{-\Gamma_2 \tau_2}$), then the spin waves are described by

$$\hat{S}_{a,l}^{(2)} = \hat{S}_a^{(2)} e^{-\Gamma_1 \tau_1} + \hat{F}_1, \quad (20)$$

$$\hat{S}_{a,l}^{(3)} = \hat{S}_a^{(3)} e^{-\Gamma_2 \tau_2} + \hat{F}_2, \quad (21)$$

where $\langle \hat{F}_1 \hat{F}_1^\dagger \rangle = 1 - e^{-2\Gamma_1 \tau_1}$ and $\langle \hat{F}_2 \hat{F}_2^\dagger \rangle = 1 - e^{-2\Gamma_2 \tau_2}$ guarantees the consistency of the operator properties of $\hat{S}_{a,l}^{(2)}$ and $\hat{S}_{a,l}^{(3)}$, respectively. The input-output relation for loss case of $\hat{a}_S^{(out)}$ becomes

$$\begin{aligned} \hat{a}_{S,l}^{(out)} = & \hat{a}_S^{(in)} \mathcal{A} + \hat{S}_a^{(in)} \mathcal{B} + \hat{a}_W^{(0)} \mathcal{C} + \hat{V}_1^\dagger \mathcal{D} + \hat{V}_2 \mathcal{E} \\ & + \hat{F}_1^\dagger \mathcal{F} + \hat{F}_2^\dagger \mathcal{G}, \end{aligned} \quad (22)$$

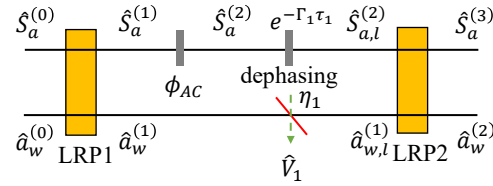
where

$$\begin{aligned} \mathcal{A} &= [\sqrt{\eta_2} G_2 G_1 + g_2 g_1 e^{i(\theta_2 - \theta_1)} (e^{-\Gamma_1 \tau_1} e^{-i\phi} + \sqrt{\eta_1}) e^{-\Gamma_2 \tau_2} / 2], \\ \mathcal{B} &= [\sqrt{\eta_2} G_2 g_1 e^{i\theta_1} + G_1 g_2 e^{i\theta_2} (e^{-\Gamma_1 \tau_1} e^{-i\phi} + \sqrt{\eta_1}) e^{-\Gamma_2 \tau_2} / 2], \\ \mathcal{C} &= g_2 e^{i\theta_2} (e^{-\Gamma_1 \tau_1} e^{-i\phi} - \sqrt{\eta_1}) e^{-\Gamma_2 \tau_2} / 2, \\ \mathcal{D} &= -g_2 e^{i\theta_2} \sqrt{1 - \eta_1} e^{-\Gamma_2 \tau_2} / \sqrt{2}, \\ \mathcal{E} &= G_2 \sqrt{1 - \eta_2}, \mathcal{F} = g_2 e^{i\theta_2} e^{-\Gamma_2 \tau_2} / \sqrt{2}, \mathcal{G} = g_2 e^{i\theta_2}. \end{aligned} \quad (23)$$

We study the effect of losses under the condition of $\theta_1 = 0$, $\theta_2 = \pi$, $\theta_\alpha = \pi/2$, and $\phi_0 = 0$ with a small ϕ_{AC} around ϕ_0 . Considering losses the terms of $\langle \hat{X}_S^{(out)} \rangle_l$, $\langle \hat{N}^{(in)} \hat{X}_S^{(out)} \rangle_l$, and $\langle \Delta^2 \hat{X}_S^{(out)} \rangle_l$ in Eq. (16) are given by

$$\langle \hat{X}_S^{(out)} \rangle_l = g_2 e^{-\Gamma_1 \tau_1} e^{-\Gamma_2 \tau_2} \kappa N_\alpha^{1/2} N_\beta, \quad (24)$$

(a) SU(2) interferometer



(b) Actively correlated atom-light hybrid interferometer

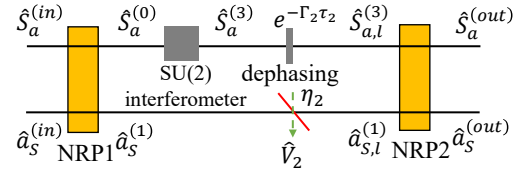


Fig. 2. A lossy interferometer model with (a) internal loss and (b) external loss.

$$\langle \hat{N}^{(in)} \hat{X}_S^{(out)} \rangle_l = g_2 e^{-\Gamma_1 \tau_1} e^{-\Gamma_2 \tau_2} \kappa N_\alpha^{1/2} N_\beta (N_\beta + 1), \quad (25)$$

and

$$\begin{aligned} & \langle \Delta^2 \hat{X}_S^{(out)} \rangle_l \\ &= (\sqrt{\eta_2} G_2 G_1 - g_2 g_1 e^{-\Gamma_1 \tau_1} e^{-\Gamma_2 \tau_2} / 2 - g_2 g_1 e^{-\Gamma_2 \tau_2} \sqrt{\eta_1} / 2)^2 \\ &+ (\sqrt{\eta_2} G_2 g_1 - G_1 g_2 e^{-\Gamma_1 \tau_1} e^{-\Gamma_2 \tau_2} / 2 - G_1 g_2 e^{-\Gamma_2 \tau_2} \sqrt{\eta_1} / 2)^2 \\ &+ g_2^2 [(1 - e^{-2\Gamma_1 \tau_1}) e^{-2\Gamma_2 \tau_2} / 2 + (1 - e^{-2\Gamma_2 \tau_2})] \\ &+ g_2^2 (2g_1^2 + 1) \kappa^2 N_\beta (N_\beta + 1) e^{-2\Gamma_1 \tau_1} e^{-2\Gamma_2 \tau_2} / 4 \\ &+ g_2^2 \kappa^2 N_\beta [N_\alpha + (N_\beta + 1) / 4] e^{-2\Gamma_1 \tau_1} e^{-2\Gamma_2 \tau_2} \\ &+ (g_2 e^{-\Gamma_2 \tau_2} \sqrt{\eta_1} / 2 - g_2 e^{-\Gamma_1 \tau_1} e^{-\Gamma_2 \tau_2} / 2)^2 \\ &+ g_2^2 (1 - \eta_1) e^{-2\Gamma_2 \tau_2} / 2 + G_2^2 (1 - \eta_2), \end{aligned} \quad (26)$$

where subscript l denotes the loss. Then the QND measurement criterion for loss case can be obtained according to Eq. (15).

In our scheme, the atomic spin wave stays in the atomic ensemble while the optical field travels out of the atomic ensemble. Here, in the short coherence time the atomic collisional dephasing loss $\Gamma_1 \tau_1$ ($\Gamma_2 \tau_2$) is very small, then we set $e^{-\Gamma_1 \tau_1} = e^{-\Gamma_2 \tau_2} = 0.9$. The correlation coefficient C as a function of η_1 and η_2 in balanced case is shown in Fig. 3. It is shown that the reduction in the correlation coefficient C increases as the loss increases. The correlation coefficient in the area of upper right corner and within the C_0 lines can be kept above 0.6. It is shown that our scheme is more tolerant with the internal photon loss compared to the photon loss outside the SU(2) interferometer. The reason behind the phenomenon is that large external photon loss affects quantum correlation between the light wave and atomic spin wave, which destroys the active correlation output readout.

In the unbalanced case ($g_1 \neq g_2$), we can adjust the gain ratio g_2/g_1 of the beam recombination process to reduce the reduction in correlation coefficient. After optimizing the g_2 , the correlation coefficient as a function of η_1 and η_2 can also be obtained, where the line with C equal to 0.6 is denoted as C_1 . The contour line of optimized g_2/g_1 as a function of η_1 and η_2 are shown in Fig. 4, where the position of C_0 (before optimization) and C_1 (after optimization) in the contour figure of the correlation coefficient versus transmission rates has changed. It is demonstrated that for a given g_1 by optimizing g_2/g_1 , the small area

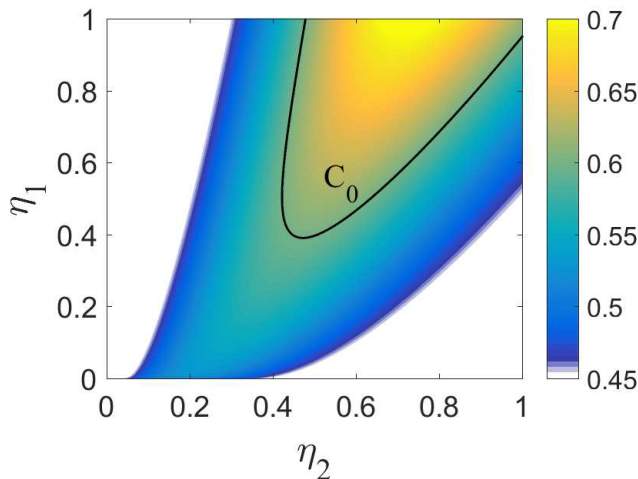


Fig. 3. Correlation coefficient C as a function of η_1 and η_2 , where $e^{-\Gamma_1\tau_1} = e^{-\Gamma_2\tau_2} = 0.9$, $\kappa = 10^{-10}$, $g_1 = g_2 = 3$, $N_\alpha = 10^{12}$, and $N_\beta = 10^8$. The correlation coefficient in the area of upper right corner and within the C_0 lines can be kept above 0.6.

between the C_0 and C_1 can still kept above 0.6. That is within a certain losses range, C can continue to beat the criteria (such as C equal to 0.6) after optimizing g_2/g_1 . The newly added area after optimization is divided into two parts, one of which is the ratio g_2/g_1 within the very small area above is less than 1, and the other part the ratio g_2/g_1 needs to be greater than 1.

4. DISCUSSION AND CONCLUSION

Our scheme can also be thought of as inserting an SU(2) interferometer into one of the arms of the SU(1,1) interferometer. Compared to a conventional SU(1,1) interferometer, the number of phase-sensing particles is further increased due to input field $\hat{a}_W^{(0)}$. In the previous scheme [32], a strong stimulated Raman process can indeed be used to excite most of the atoms to the $|m\rangle$ state to improve the number of phase-sensing particles. However, this will produce additional nonlinear effects and noise light fields [39–41]. Therefore, in the current scheme, firstly a spontaneous Raman process is used, and then a LRP is used to generate the Rabi-like superposition oscillation between light and the atom. By controlling the interaction time, more atoms can be generated to the $|m\rangle$ state to improve the number of phase-sensing particles to enhance the QND measurement.

Based on the previous experimental works [28, 29], the actively correlated atom-light hybrid interferometer could be implemented in the rubidium atomic system. Moreover, the scheme is a multi-arm interferometer and it provides an option for the simultaneous estimation of more than two parameters with a wide range of applications, such as phase imaging [42], quantum sensing networks [43], the detection of vector fields [44] and so on.

In conclusion, we have proposed an actively correlated atom-light hybrid interferometer and used it for QND measurement of photon number via the AC-Stark effect. In the scheme, the atomic spin wave of the SU(2) interferometer is prepared via a NRP and the output is detected with the method of active correlation readout via another NRP. Benefiting from that,

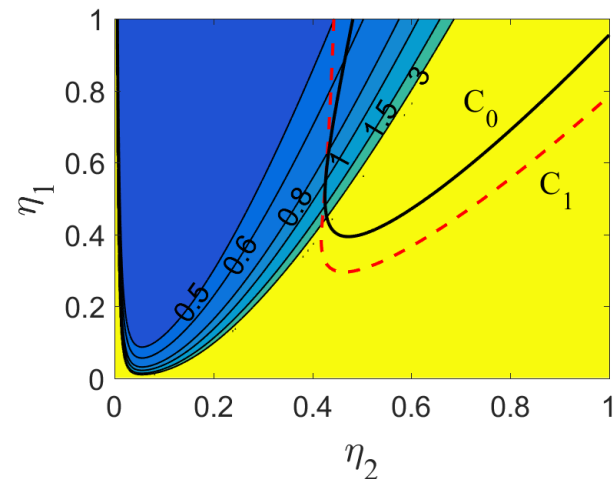


Fig. 4. Contour line of optimized g_2/g_1 as a function of η_1 and η_2 with $e^{-\Gamma_1\tau_1} = e^{-\Gamma_2\tau_2} = 0.9$, where $\kappa = 10^{-10}$, $g_1 = 3$, $N_\alpha = 10^{12}$, and $N_\beta = 10^8$. The correlation coefficient in the area of upper right corner and within the line C_0 (before optimization) or C_1 (after optimization) can be kept above 0.6.

the SNR in the balanced case is improved by a factor of g compared to the traditional SU(2) interferometer. The condition for a perfect correlation is given. The measurement quality is reduced in the presence of losses. We can adjust the gain parameter of the NRP in readout stage to reduce the impact of losses.

FUNDING

This work is supported by Development Program of China Grant No. 2016YFA0302001; National Natural Science Foundation of China Grants No. 11974111, No. 11874152, No. 91536114, No. 11574086, No. 11974116, No. 11654005; Shanghai Rising-Star Program Grant No. 16QA1401600; the Shanghai talent program, and the Fundamental Research Funds for the Central Universities.

DISCLOSURES

The authors declare no conflicts of interest.

REFERENCES

1. C. M. Caves, K. S. Thorne, R. W. P. Drever, V. D. Sandberg and M. Zimmermann, "On the measurement of a weak classical force coupled to a quantum-mechanical oscillator. I. Issues of principle," *Rev. Mod. Phys.* **52**, 341-392 (1980).
2. V. B. Braginsky and F. Ya. Khalili, "Quantum nondemolition measurements: The route from toys to tools," *Rev. Mod. Phys.* **68**, 1-11 (1996).
3. F. Lecocq, J. B. Clark, R. W. Simmonds, J. Aumentado, and J. D. Teufel, "Quantum Non-Demolition Measurement of a Nonclassical State of a Massive Object," *Phys. Rev. X* **5**, 041037 (2015).
4. M. Rossi, D. Mason, J. Chen, Y. Tsaturyan, and A. Schliesser, "Measurement-Based Quantum Control of Mechanical Motion," *Nature (London)* **563**, 53-58 (2018).
5. D. B. Hume, T. Rosenband, and D. J. Wineland, "High-Fidelity Adaptive Qubit Detection through Repetitive Quantum Non-Demolition Measurements," *Phys. Rev. Lett.* **99**, 120502 (2007).
6. F. Wolf, Y. Wan, J. C. Heip, F. Gebert, C. Shi, and P. O. Schmidt, "Non-Destructive State Detection for Quantum Logic Spectroscopy of Molecular Ions," *Nature (London)* **530**, 457-460 (2016).

7. M. Raha, S. Chen, C. M. Phenicie, S. Ourari, A. M. Dibos, and J. D. Thompson, "Optical Quantum Non-Demolition Measurement of a Single Rare Earth Ion Qubit," *Nat. Commun.* **11**, 1-6 (2020).

8. X. Xue, B. D'Anjou, T. F. Watson, D. R. Ward, D. E. Savage, M. G. Lagally, M. Friesen, S. N. Coppersmith, M. A. Eriksson, W. A. Coish, and L. M. K. Vandersypen, "Repetitive Quantum Non-Demolition Measurement and Soft Decoding of a Silicon Spin Qubit," *Phys. Rev. X* **10**, 021006 (2020).

9. S. Hacohen-Gourgy, L. S. Martin, E. Flurin, V. V. Ramasesh, K. B. Whaley, and I. Siddiqi, "Quantum Dynamics of Simultaneously Measured Non-Commuting Observables," *Nature (London)* **538**, 491-494 (2016).

10. U. Vool, S. Shankar, S. O. Mundhada, N. Ofek, A. Narla, K. Sliwa, E. Zalys-Geller, Y. Liu, L. Frunzio, R. J. Schoelkopf, S. M. Girvin, and M. H. Devoret, "Continuous Quantum Non-Demolition Measurement of the Transverse Component of a Qubit," *Phys. Rev. Lett.* **117**, 133601 (2016).

11. A. Reiserer, S. Ritter, and G. Rempe, "Non-Destructive Detection of an Optical Photon," *Science* **342**, 1349-1351 (2013).

12. S. Kono, K. Koshino, Y. Tabuchi, A. Noguchi, and Y. Nakamura, "Quantum Non-Demolition Detection of an Itinerant Microwave Photon," *Nat. Phys.* **14**, 546-549 (2018).

13. N. Imoto, H. A. Haus, and Y. Yamamoto, "Quantum nondemolition measurement of the photon number via the optical Kerr effect," *Phys. Rev. A* **32**, 2287-2292 (1985).

14. M. J. Holland, D. F. Walls, and P. Zoller, "Quantum nondemolition measurements of photon number by atomic beam deflection," *Phys. Rev. Lett.* **67**, 1716-1719 (1991).

15. S. R. Friberg, S. Machida, and Y. Yamamoto, "Quantum-nondemolition measurement of the photon number of an optical soliton," *Phys. Rev. Lett.* **69**, 3165-3168 (1992).

16. K. Jacobs, P. Tombesi, M. J. Collett, and D. F. Walls, "Quantum-nondemolition measurement of photon number using radiation pressure," *Phys. Rev. A* **49**, 1961-1966 (1994).

17. Y. Sakai, R. J. Hawkins, and S. R. Friberg, "Soliton-collision interferometer for the quantum nondemolition measurement of photon number: numerical results," *Opt. Lett.* **15**, 239-241 (1990).

18. P. Kok, H. Lee and J. P. Dowling, "Single-photon quantum-nondemolition detectors constructed with linear optics and projective measurements," *Phys. Rev. A* **66**, 063814 (2002).

19. C. C. Gerry and T. Bui, "Quantum non-demolition measurement of photon number using weak nonlinearities," *Phys. Lett. A* **372**, 7101-7104 (2008).

20. W. J. Munro, K. Nemoto, R. G. Beausoleil, and T. P. Spiller, "High-efficiency quantum-nondemolition single-photon-number-resolving detector," *Phys. Rev. A* **71**, 033819 (2005).

21. G. Nogues, A. Rauschenbeutel, S. Osnaghi, M. Brune, J. M. Raimond, and S. Haroche, "Seeing a single photon without destroying it," *Nature (London)* **400**, 239-242 (1999).

22. Y. F. Xiao, S. K. Ozdemir, V. Gaddam, C. H. Dong, N. Imoto, and L. Yang, "Quantum nondemolition measurement of photon number via optical Kerr effect in an ultra-high-Q microtoroid cavity," *Opt. Express* **16**, 21462-21475 (2008).

23. M. Ludwig, A. H. Safavi-Naeini, O. Painter, and F. Marquardt, "Enhanced Quantum Nonlinearities in a Two-Mode Optomechanical System," *Phys. Rev. Lett.* **109**, 063601 (2012).

24. D. Malz and J. I. Cirac, "Nondestructive photon counting in waveguide qed," *Phys. Rev. Research* **2**, 033091 (2020).

25. J. Liu, H. T. Chen and D. Segal, "Quantum nondemolition photon counting with a hybrid electromechanical probe," *Phys. Rev. A* **102**, 061501(R) (2020).

26. J. Jacobson, G. Björk and Y. Yamamoto, "Quantum limit for the atom-light interferometer," *Appl. Phys. B* **60**, 187-191 (1995).

27. G. Campbell, M. Hosseini, B. M. Sparkes, P. K. Lam, and B. C. Buchler, "Time-and frequency-domain polariton interference," *New J. Phys.* **14**, 033022 (2012).

28. B. Chen, C. Qiu, S. Chen, J. Guo, L. Q. Chen, Z. Y. Ou, and W. Zhang, "Atom-light hybrid interferometer," *Phys. Rev. Lett.* **115**, 043602 (2015).

29. C. Qiu, S. Chen, L. Q. Chen, B. Chen, J. Guo, Z. Y. Ou, and W. Zhang, "Atom-light superposition oscillation and Ramsey-like atom-light interferometer," *Optica* **3**, 775-780 (2016).

30. H.-M. Ma, D. Li, C.-H. Yuan, L. Q. Chen, Z. Y. Ou, and W. Zhang, "SU (1, 1)-type light-atom-correlated interferometer," *Phys. Rev. A* **92**, 023847 (2015).

31. Z.-D. Chen, C.-H. Yuan, H.-M. Ma, D. Li, L. Q. Chen, Z. Y. Ou, and W. Zhang, "Effects of losses in the atom-light hybrid SU (1, 1) interferometer," *Opt. Express* **24**, 17766-17778 (2016).

32. S. Y. Chen, L. Q. Chen, Z. Y. Ou, and W. Zhang, "Quantum non-demolition measurement of photon number with atom-light interferometers," *Opt. Express* **25**, 31827-31839 (2017).

33. D. H. Fan, S. Y. Chen, Z. F. Yu, K. Zhang and L. Q. Chen, "Quality estimation of non-demolition measurement with lossy atom-light hybrid interferometers," *Opt. Express* **28**, 9875-9884 (2020).

34. J. Aasi *et al.*, "Advanced LIGO," *Classical Quantum Gravity* **32**, 074001 (2015).

35. M. J. Holland, M. J. Collett, D. F. Walls, and M. D. Levenson, "Nonideal quantum nondemolition measurements," *Phys. Rev. A* **42**, 2995-3005 (1990).

36. S. H. Autler and C. H. Townes, "Stark effect in rapidly varying fields," *Phys. Rev.* **100**, 703-722 (1955).

37. K. Hammerer, A. S. Sørensen and E. S. Polzik, "Quantum interface between light and atomic ensembles", *Rev. Mod. Phys.* **82**, 1041-1093 (2010).

38. G.-F. Jiao, K. Zhang, L. Q. Chen, W. Zhang and C.-H. Yuan, "Nonlinear phase estimation enhanced by an actively correlated Mach-Zehnder interferometer," *Phys. Rev. A* **102**, 033520 (2020).

39. M. Dabrowski, R. Chrapkiewicz, and W. Wasilewski, "Hamiltonian design in readout from room-temperature Raman atomic memory," *Opt. Express* **22**, 26076-26091 (2014).

40. J. Nunn, J. H. D. Munns, S. Thomas, K. T. Kaczmarek, C. Qiu, A. Feizpour, E. Poem, B. Brecht, D. J. Saunders, P. M. Ledingham, D. V. Reddy, M. G. Raymer, and I. A. Walmsley, "Theory of noise suppression in Δ -type quantum memories by means of a cavity," *Phys. Rev. A* **96**, 012338 (2017).

41. S. E. Thomas, T. M. Hird, J. H. D. Munns, B. Brecht, and D. J. Saunders, "Raman quantum memory with built-in suppression of four-wave-mixing noise," *Phys. Rev. A* **100**, 033801 (2019).

42. M. Tsang, "Quantum imaging beyond the diffraction limit by optical centroid measurements," *Phys. Rev. Lett.* **102**, 253601 (2009).

43. T. J. Proctor, P. A. Knott, and J. A. Dunningham, "Multiparameter estimation in networked quantum sensors," *Phys. Rev. Lett.* **120**, 080501 (2018).

44. T. Baumgratz and A. Datta, "Quantum Enhanced Estimation of a Multidimensional Field," *Phys. Rev. Lett.* **116**, 030801 (2016).